J Fluoresc (2014) 24:1389–1396
DOI 10.1007/s10895-014-1411-2

ORIGINAL PAPER

Interaction of One Anthraquinone Derivative with ctDNA Analyzed by Spectroscopic and Modeling Methods

Yanrui Cui · Zheng Fu · Shaoguang Geng · Guisheng Zhang · Fengling Cui

Received: 3 April 2014 / Accepted: 19 May 2014 / Published online: 24 June 2014

Abstract The interaction of one anthraquinone derivative (AOMan) with calf thymus deoxyribonucleic acid (ctDNA) was systematically investigated at physiological pH 7.4 by fluorescence spectroscopy and molecular modeling. Binding constants of ctDNA with AOMan were calculated at different temperatures. Thermodynamic parameters, enthalpy and entropy changes were calculated according to Van't Hoff equation, which indicated that the reaction was spontaneous and predominantly enthalpically driven. The increasing viscosity of ctDNA indicated that AOMan could intercalate into the base pairs of ctDNA. This conclusion was also demonstrated by the results obtained from KI quenching, denatured DNA studies and fluorescence polarization experiment. Furthermore, the molecular modeling results showed that anthraquinone ring tended to slide into the G–C rich region of ctDNA through the hydrogen bond, which are consistent with the results from experimental methods. Studying the binding interaction of target anthraquinones with DNA is one of the key steps in their DNA-changing action and the design of new drugs.

Keywords Calf thymus DNA (ctDNA) · Anthraquinone derivative (AOMan) · Fluorescence spectroscopy · Molecular docking · Interaction

Introduction

Anthraquinone is one of the most abundant of all kinds of natural quinone compounds. Initially, anthraquinones are used as natural dyes. Then anthraquinones arouse increasing attention on account of profuse medicinal values such as antibacteria and anti-inflammator, antiviral, anticancer, cholagogue, nootropic, anti-aging, antimutagenesis, anti-ultraviolet etc. Additionally, anthraquinones are proved to have hemostasis, promoting sleep quality, reducing blood fat and enhancing immunity activities. Based on the above-said characteristics, anthracycline antibiotics are widely used in the cancer treatment. However, the side effects especially serious cardiotoxicity and mutiple drug resistance limit their application in clinic greatly. Thus, modifying the structure of anthracycline antibiotics has become the main means and approach to develop new drugs with no resistance and lower cardiotoxicity. With further research of anthraquinone drug reaction targets [1, 2], drug resistance and cardiotoxicity, structure-activity relationship can be achieved for constructing and synthesizing rational anthracycline antibiotic derivates, which provides the theory support in researching high-activity and hypotoxicity anthracycline antibiotic drugs by structural optimization. AOMan (Fig. 1) is a one anthraquinone derivative, which exhibits potent antitumor activities in drug-sensitive and drug-resistant cell lines. The compound AOMan is worthy of further evaluations as a new drug candidate.

DNA is in the form of a double helix present in body, where each strand is composed of four major types of nucleotide (adenine, guanine, thymine and cytimidine) and it is connected by phosphodiester bond [3]. It carries most hereditary information and facilitates the biological synthesis of enzymes and proteins through replication and transcription of this information [4]. The binding of small molecules to DNA involves electrostatic interaction [5], intercalation between base pairs [6] and minor and major DNA grooves binding interaction [7]. Previous studies reveal that anthraquinones can prevent cancer cells from multiplying by intercalating with DNA that inhibit DNA replication and RNA transcription [8], so it is

Y. Cui · Z. Fu · S. Geng · G. Zhang · F. Cui (✉)
School of Chemistry and Chemical Engineering, Key Laboratory of Green Chemical Media and Reactions, Ministry of Education, Henan Normal University, Xinxiang 453007, China
e-mail: fenglingcui@hotmail.com

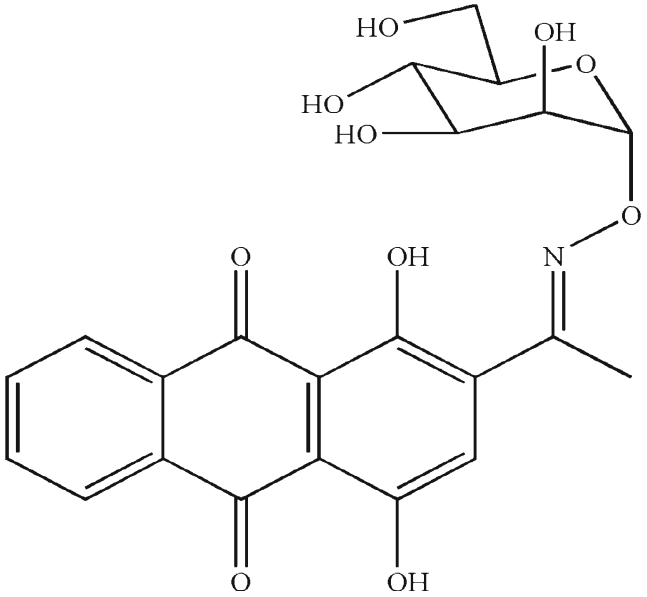

Fig. 1 The molecular structure of AOMan ($C_{22}H_{21}NO_{10}$, molecular weight: 459.40)

of great significance to investigate the interaction between the anthraquinones and DNA to further clearly make the mechanism of binding interaction [9]. In addition, studying the binding interaction of target anthraquinones with DNA is one of the key steps in their DNA-changing action and the new drugs designing.

In this work, we introduce a simple method for investigating the mechanism of interaction—Fluorescence method which have been used widely in research [10–13]. By understanding the mechanism of interaction, designing of new DNA-targeted drugs and the screening of these in vitro will be possible [14]. In present studies interaction of AOMan with calf thymus DNA (ctDNA) is investigated by fluorescence spectroscopy combine with the determination of series of thermodynamic parameters, binding constants, viscosity and molecular modeling techniques.

Experimental

Materials

AOMan was synthesized in the laboratory (5.877×10^{-5} mol L^{-1}). ^{1}H NMR (400 MHz, DMSO-d_6) (ppm): 13.26 (1H, s), 12.56 (1H, s), 8.26–8.29 (2H, m), 7.99–8.01 (2H, m), 7.37 (1H, s, H-3), 5.37 (1H, s), 5.02 (1H, d, J=4.0), 4.82 (1H, d, J=5.6), 4.73 (1H, d, J=5.6), 4.52 (1H, t, J=6.0), 4.36 (1H, t), 3.85 (1H, s), 3.63–3.68 (1H, m), 3.44–3.50 (3H, m), 2.26 (3H, s, H-12). ^{13}C NMR (100 MHz, DMSO-d_6) (ppm): 187.5, 186.9, 156.0, 155.8, 155.3, 136.8, 135.6, 133.2, 128.0, 127.2, 127.1, 113.8, 113.7, 103.0, 75.6, 71.8, 69.5, 67.2, 61.5, 15.7. ctDNA was obtained from the Sigma Company (Sigma-Aldrich, USA) and used without further purification, the stock solution of ctDNA was prepared by dissolving solid ctDNA in doubly distilled water and stored at 4 °C. The concentration of ctDNA was determined by absorption spectroscopy using the molar extinction coefficient of 6600 M^{-1} cm^{-1} at 260 nm [15, 16]. The purity of ctDNA was verified by monitoring the ratio of absorbance at 260 nm to 280 nm (more than 1.8) [17–19]. The acidity of the solutions (pH 7.4) were controlled by Tris–HCl buffer solution and 2×10^{-2} mol L^{-1} KI solution was prepared before the experiment.

DNA used in this work was double stranded DNA (dsDNA) unless specified. All other reagents were at least analytical reagent grade. Doubly distilled water was used throughout.

Apparatus

The pH value of the solutions was determined with a PFS-80 pF-meter (Shanghai Dazhong Analytical Instrument Plant, Shanghai, China). The fluorescence spectra were carried out on a Cary Eclipse fluorescence spectrophotometer equipped with quartz cells of 1 cm path length (VARIAN, USA) and thermostatically controlled by a SHP DC-0515 thermostatic bath (Shanghai Hengping Sciences Instrument Co. Ltd., Shanghai, China). Viscometric measurements were conducted by using an Ubbelohde viscometer and the flow time of the solution through the capillary was measured with a digital stopwatch.

Experimental Procedures

Fluorescence Measurement

2.0 mL pH 7.4 of Tris–HCl buffer solution, a constant volume of AOMan and vary volume of ctDNA solution were added into the 10 mL volumetric tubes, and the mixed solution was diluted to the final volume with doubly distilled water. In order to evaluate the effect of temperature on AOMan-ctDNA interaction, the fluorescence spectra were recorded at three different temperatures (290, 301 and 310 K). The fluorescence measurement was performed with the excitation wavelength at 254 nm and the emission was changed from 525–750 nm with the slit widths both were 5 nm.

Effect of Ionic Strength

A series of assay solutions containing fixed amount of AOMan and various amounts of NaCl were prepared to investigate the influence on fluorescent intensity of AOMan. Another series of assay solutions containing fixed amount of AOMan–ctDNA were prepared to investigate the influence on fluorescent intensity of AOMan–ctDNA.

Viscosity Studies

The viscosity of the ctDNA solution was measured at 25± 0.1 °C using an Ubbeholde viscometer and the concentration of ctDNA was kept at 5×10^{-5} mol L^{-1}, while various concentration of AOMan was added into the viscometer to give a certain R (R=[AOMan]/[ctDNA]=0–0.25) value. The relative specific viscosity $(\eta/\eta_0)^{1/3}$ was plotted against binding ratio R, according to the theory of Cohen and Eisenberg [20]. Where η_0 was the viscosity of the ctDNA solution alone and η was the viscosity of ctDNA solutions when presence of AOMan [21]. Viscosity values were calculated from the observed flow time of ctDNA containing solutions (t) and corrected for buffer solution (t_0), using $\eta=(t\text{-}t_0)/t_0$ [22]. Each point measured was the average of three readings.

Denatured DNA Studies

The denatured DNA (ssDNA) was obtained by heating native dsDNA in a boiling water bath for 30 min and followed by rapidly cooling in an ice-water bath for 10 min [23]. The interaction mode was studied by comparison of the quenching effects of ssDNA and dsDNA on the fluorescence intensity of AOMan.

Iodide Quenching Studies

Fluorescence quenching studies were discussed by gradually adding the anionic quencher solution (KI) to AOMan and AOMan − ctDNA complex solutions. The quenching constants were calculated and then compared for studying the interaction mode of ctDNA with AOMan.

Fluorescence Polarization Experiment

A series of assay solutions containing fixed amount of AOMan and various amounts of ctDNA (The concentration of ctDNA changed from 0 to 5.0×10^{-5} mol L^{-1}) were prepared to investigate the influence on fluorescence polarization of AOMan.

Molecular Modeling Studies

Docking studies were carried out using generated by Sybyl 6.9 docking software. Structure of B-DNA 425D was taken from protein data bank for performing docking [24]. The 3D structure of DNA was formed according to the Amber 4.0 force field with Kollman-all-atom charges. Before the docking running, the structure of AOMan was generated by Sybyl 6.9 and subsequently optimized to minimal energy with the help of the Tripos force field using Gasteiger–Marsili charges. The water was removed from the macromolecule file, polar hydrogen atoms and Gasteiger charges were added. The possible conformation of the AOMan bound to DNA was calculated by the FlexX software of the Sybyl suite.

Results and Dicussion

Fluorescence Spectral Studies

Fluorescence spectroscopy was used for characterizing the binding characteristics of the AOMan with DNA [25]. The compound AOMan could emit luminescence in Tris–HCl buffer in the area from 525 to 750 nm with maximum wavelength about 585 nm. Figure 3 is the fluorescence spectra of AOMan in absence and presence of variational amounts of ctDNA. From the Fig. 3, it could be seen that with the addition of ctDNA, the fluorescence intensity of AOMan was decrease. The change of fluorescence emission intensities indicated that interaction existing between AOMan and ctDNA [26].

Fluorescence Quenching Studies

Quenching mechanism is usually divided into static and dynamic. The collision of excited lumophore and the quencher can form dynamic quenching. The rate of dynamic quenching is a diffusion-controlled process, and factors that affect it include the temperature and viscosity of the solution [27]. As above, the other form of quenching is static quenching, which indicates that the fluorophore and the quencher form a nonfluorescent ground-state complex [20]. Static and dynamic quenching can be distinguished by temperature. The stability of complex can be decrease with the temperature increasing, and the static quenching constants will be decrease. In contrast, higher temperatures lead to larger diffusion coefficients, the dynamic quenching constants can be increased with rising the temperature.

In order to study the quenching mechanism of AOMan by ctDNA, the Stern–Volmer equation was used [28–30]:

$$\frac{F_0}{F} = 1 + K_q\tau_0[Q] = 1 + K_{SV}[Q] \quad (1)$$

where F_0 is the fluorescence intensity in the absence of the quencher; F is the fluorescence intensity in the presence of the quencher, [Q] is the concentration of the quencher; K_q is the biomolecule quenching rate constant; K_{SV} signifies the Stern-Volmer quenching constant; τ_0 is the average lifetime of the molecule without the quencher and its value is about 10^{-8} s [31].

The K_{SV} of AOMan by ctDNA at different temperatures (290, 301 and 310 K) was obtained by linear regression of a plot of F_0/F against [Q] (Fig. 2). The K_{SV} decrease with

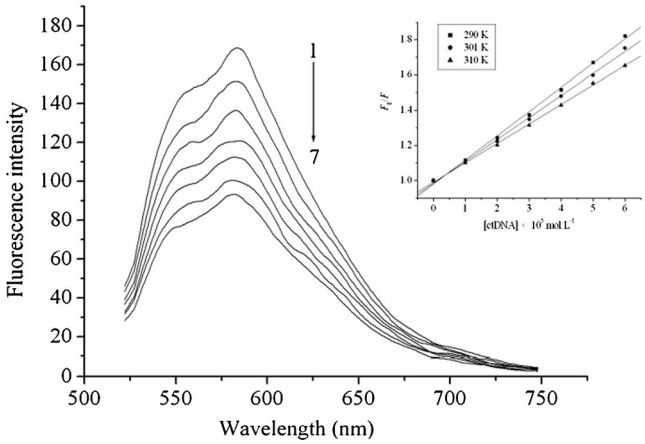

Fig. 2 Fluorescence spectra of AOMan in the absence and presence of ctDNA. C_{ctDNA}=0, 1.0, 2.0, 3.0, 4.0, 5.0 and 6.0×10^{-5} mol L^{-1}; C_{AOMan}= *2.35× 10^{-6} mol L^{-1}. The inset is Stern–Volmer curves for the binding of AOMan to ctDNA at different temperatures*

temperature rising showed that ctDNA can quench the fluorescence of AOMan by a static quenching procedure [32]. τ_0 was about 10^{-8} s, and the bimolecular quenching constants K_q were obtained and listed in Table 1. The values of K_q were larger than the limiting diffusion rate constant of biomolecule (2.0×10^{10} L mol^{-1} s^{-1}), which also indicated the static quenching occurs in the process of AOMan quenching by ctDNA [33].

Binding and Thermodynamic Parameters Characteristics of Interactions

The binding constant (K) and binding sites (n) were calculated using equation [34]:

$$\log\frac{F_0-F}{F} = \log K + n\log[Q] \quad (2)$$

K and n could be determined by the intercept and slope of double logarithm regression curve of log $(F_0$-$F)/F$ versus log $[Q]$ based on the equation (Fig. 3). Table 2 listed the K of AOMan-ctDNA at different temperatures, which suggested that the binding constants decreased with temperature rising. The results indicated that AOMan interacted with ctDNA form an unstable compound, the stability of the compounds decreases with the temperature increasing. The values of n are close to 1, which proves that molecule of AOMan binds to a single site of ctDNA.

The non-covalent interactions between small molecules and biomolecules include hydrogen bond, electrostatic forces, van der Waals forces, and hydrophobic interaction. When small molecules bind with DNA through minor groove binding, hydrogen bonds will play an important role in the process. However, when small molecules bind with DNA through intercalation, hydrophobic interactions and van der Waals forces will play an important role [27]. If the enthalpy change does not vary obviously at different temperatures, enthalpy change (ΔH) and entropy change (ΔS) can be determined from the van't Hoff equation:

$$\ln K = -\Delta H/RT + \Delta S/R \quad (3)$$

Where R is gas constant; K is the binding constant (they are studied at 290, 301 and 310 K). The values of ΔS and ΔH are obtained from the intercept and slope of the linear plot based on ln$K$ versus 1/T. The free energy change (ΔG) can be calculated from the below equation:

$$\Delta G = \Delta H - T\Delta S = -RT\ln K \quad (4)$$

The thermodynamic parameters for the interaction of AOMan with ctDNA were listed in Table 2. The value of ΔH was −28.77 kJ mol^{-1} and the value of ΔS was −11.17 J mol^{-1} K^{-1}, which suggested that van der Waals forces and hydrogen bonds played an important role in the process of the binding between AOMan and ctDNA [35], and the mode of binding was intercalation. ΔH <0 and ΔG <0 indicated that the interaction process was a spontaneous and predominantly enthalpically driven reaction.

Effect of Ionic Strength

Investigating the change of spectra with different ionic strength is also a useful method to study the binding modes between molecules and DNA. DNA is an anionic polyelectrolyte with phosphate groups and NaCl is usually used for

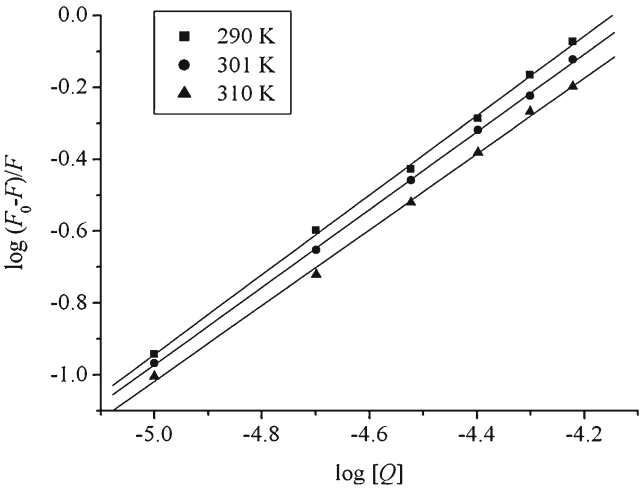

Fig. 3 Double logarithmic curves of ctDNA quenching the fluorescence of AOMan

Table 1 The Stern-Volmer quenching constant K_{SV} and the quenching rate constants K_q at different temperatures

T (K)	Stern-Volmer equation	K_{SV} (L mol^{-1})	K_q (L mol^{-1} s^{-1})	R
290	Y=0.9759+1.406×10^4[Q]	1.406×10^4	1.406×10^{12}	0.9978
301	Y=0.9838+1.248×10^4[Q]	1.248×10^4	1.248×10^{12}	0.9988
310	Y=0.9891+1.074×10^4[Q]	1.074×10^4	1.074×10^{12}	0.9991

controlling the ionic strength of the solutions. Na^+ can compete for phosphate groups of DNA, so addition of Na^+ will weaken the electrostatic interaction between molecules and DNA. Figure 4 is the change of fluorescence intensity of AOMan and AOMan-ctDNA system, displaying that ionic strength had little effect on fluorescence intensity of these systems. The result suggested that the binding of AOMan to ctDNA could exclude electrostatic binding mode [36].

Viscosity Studies

Viscosity studies are regarded as the most critical and credible test for elucidating the binding mode of small molecules to DNA in solution [37]. To further clarify the binding of the AOMan and ctDNA, viscosity measurements are carried out by varying the concentration of the AOMan in ctDNA solution. Figure 5 shows that the viscosity of the ctDNA solution obviously increases with the addition of the AOMan, which provided a strong evidence for intercalation. Because AOMan intercalated into ctDNA making the effective ctDNA length increase, leading to the viscosity increase of ctDNA. In contrast, complexes that binding with the DNA by groove binding or non classical intercalation, under the same conditions, cause less positive or negative or no changes in DNA solution viscosity [38].

The fluorescence measurements for the binding of AOMan with ssDNA were carried out under the same conditions as that with dsDNA. A small molecule intercalates between base pairs of ctDNA, the quenching effect of ssDNA should be weaker than that of dsDNA for the release of the double strands of DNA; the quenching effect of ssDNA should be strengthened in comparison to dsDNA through groove binding; the quenching effect should be the same when interacted with the phosphate groups of DNA [39, 40].

From the Fig. 6, it could be seen that the binding constant of AOMan-ssDNA was smaller than that of AOMan-dsDNA. Apparently, the binding mode of AOMan and ctDNA was relevant to the double helix of ctDNA. It was reasonable that the intercalative binding was the major binding mode for AOMan to ctDNA from the results.

Iodide Quenching Studies

The KI quenching experiments support further evidence for the intercalative binding of AOMan to ctDNA. The fluorescence of small molecule can effectively quenched by KI, the change of the fluorescence in the absence and presence of ctDNA can deduce the binding mode of the small molecule with ctDNA. If small molecules intercalate to DNA, the small molecules will protect from being quenched by anionic quencher. However, if the small molecules bind to DNA by groove binding, the small molecules should be quenched readily by anionic quenchers. Figure 7 was the quenching behavior of KI in the AOMan and AOMan-ctDNA systems were investigated. The results showed that iodide quenching effect was decreased when AOMan was bound to ctDNA, suggesting that an intercalation binding should be the interaction mode of AOMan with DNA [35].

Fluorescence Polarization Experiment

Fluorescence polarization experiment can also provide an effective parameter for investigating the binding mode of AOMan with ctDNA in different microenvironments. Fluorescence polarization can be obtained from the equation below [41]:

$$P = (I_{VV} - GI_{VH})/(I_{VV} + GI_{VH}) \quad (5)$$

where P represents fluorescence polarization, I_{VV} and I_{VH} are the vertical polarization intensity vertical with excitation and the horizontal polarization intensity vertical with excitation, respectively; I_{HV} and I_{HH} are the vertical polarization intensity parallel with excitation and the horizontal polarization intensity parallel with excitation respectively; G is the corrected

Table 2 The binding constants, number of binding sites and thermodynamic parameters of the interaction of AOMan with ctDNA at various temperatures

T (K)	K (L mol^{-1})	n	ΔG (kJ mol^{-1})	ΔH (kJ mol^{-1})	ΔS (J mol^{-1} K^{-1})
290	3.889×10^4	1.106	−25.53		
301	2.683×10^4	1.080	−25.41	−28.77	−11.17
310	1.790×10^4	1.054	−25.31		

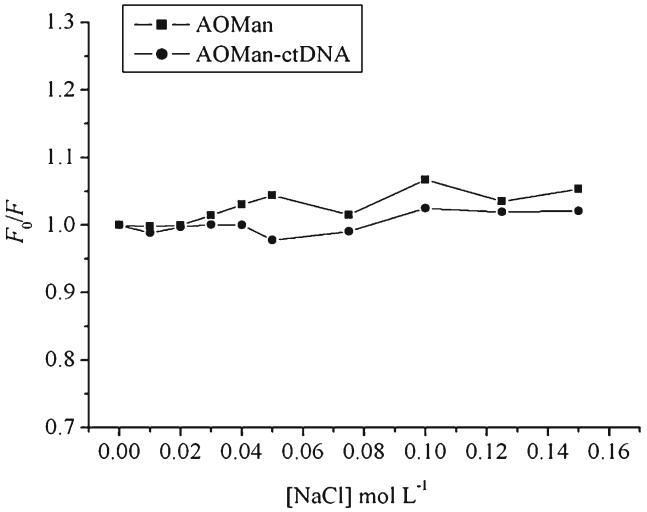

Fig. 4 Effect of NaCl on the fluorescence intensity of AOMan and AOMan-ctDNA system. Conditions: (■) in the absence of ctDNA; (●) in the presence of 1×10^{-6} mol L^{-1} ctDNA; $C_{AOMan}=1.18\times10^{-6}$ mol L^{-1}

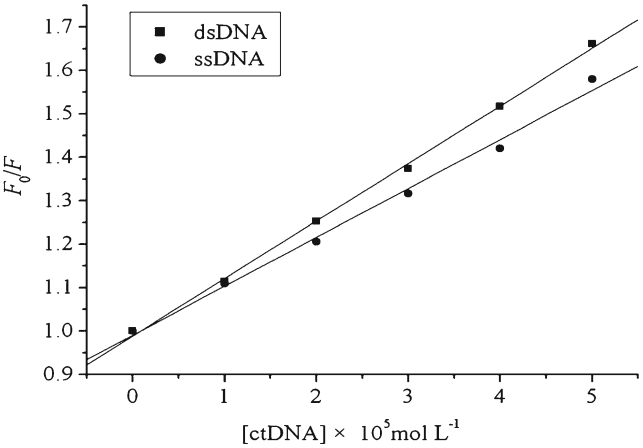

Fig. 6 Effect of dsDNA and ssDNA on the AOMan fluorescence intensity, $C_{AOMan}=2.35\times10^{-6}$ mol L^{-1}

factor and equal to I_{HV}/I_{HH}. Fluorescence polarization of small molecule is low in solution, and will be changed when interacting with DNA. If the polarization changed a little, the binding may belong to groove or other binding modes. On the contrary, if the chromophore of small molecule intercalates into the helix, its rotational motion should be restricted and therefore the fluorescence polarization should be increased evidently [42]. Figure 8 shows an obvious enhancement of polarization which is observed in the AOMan-ctDNA system. Fluorescence polarization on binding AOMan to ctDNA supported the intercalation of AOMan into the helix [43].

Molecular Modeling Studies

Molecular docking studies are used for getting insight into the interaction between ctDNA and AOMan. The docking results were shown in Fig. 9, which suggested that the chromophore of AOMan could slide into the G–C rich region of ctDNA. In addition, there were some hydrogen interactions between ADOX and ctDNA, the H atom of G-5 was at a distance of 1.78 Å from phenolic hydroxyl O atom of AOMan, the O atom of C-21 was at a distance of 2.07 Å from phenolic hydroxyl H atom of AOMan, the H atom of G-4 was at a distance of 2.09 Å from nitrogen atom of AOMan, the O atoms of sugar ring of AOMan was at a distance of 2.01 and 2.12 Å from G-22 and G-23, respectively. These results further confirm that the interaction mode between AOMan and ctDNA was intercalation dominated and hydrogen bonding forces might play an essential role in the binding. This also indicated that results were approximately in agreement with the above spectroscopic analysis, and molecular modeling could mutually provide fruitful information about the mechanism of interaction from different aspects.

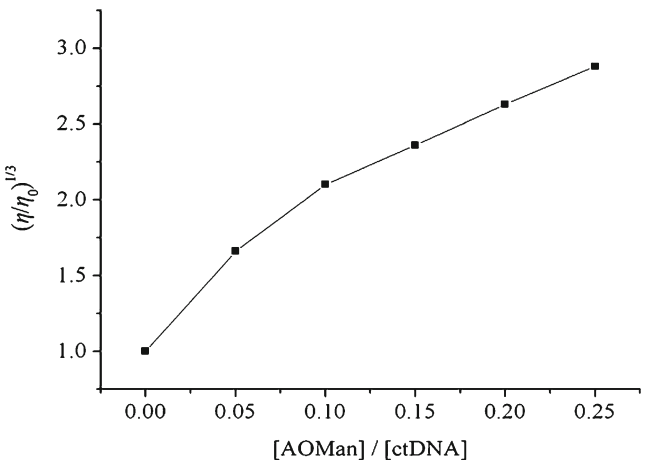

Fig. 5 Effect of increasing amount of AOMan on the relatively viscosity of ctDNA. Denatured DNA studies

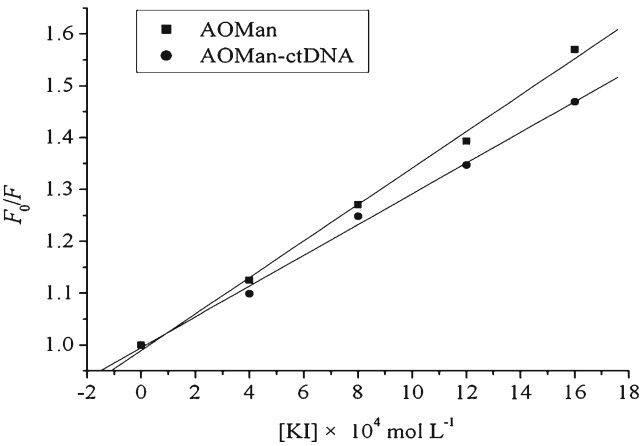

Fig. 7 Fluorescence quenching plots of AOMan by KI in the absence and presence of ctDNA. $C_{ctDNA}=5\times10^{-6}$ mol L^{-1}, $C_{AOMan}=1.18\times10^{-6}$ mol L^{-1}

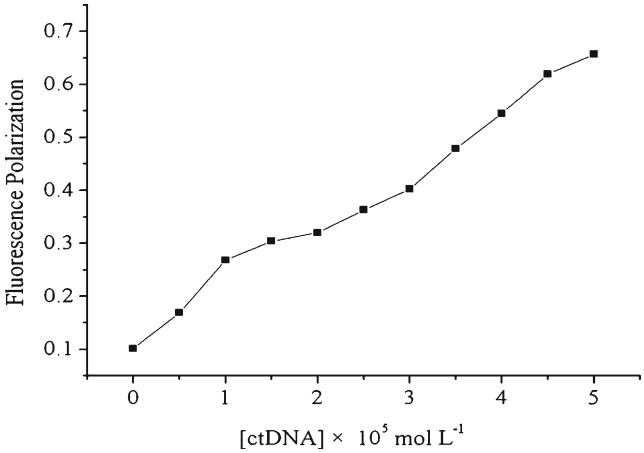

Fig. 8 Influence of ctDNA concentration on fluorescence polarization of AOMan. C_{AOMan}=2.18×10^{-6} mol L^{-1}, C_{ctDNA}=0, 0.5, 1.0, 1.5, 2.0, 2.5, 3.0, 3.5, 4.0, 4.5, 5.0×10^{-5} mol L^{-1}

Conclusion

In this paper, the interaction of AOMan with ctDNA was investigated by fluorescence spectroscopy and molecular modeling. The effect of ionic strength showed that the addition of NaCl could not affect the binding of AOMan and ctDNA, which confirmed the binding mode of AOMan with ctDNA was intercalation. Fluorescence polarization and denatured DNA studies also applied to demonstrate that AOMan molecule was intercalates between the base pairs of ctDNA. In addition, Iodide quenching studies indicated that K_{SV} value for the bound AOMan with ctDNA was lower than the free AOMan. Moreover, the results obtained from molecular docking corroborated with which obtained from spectroscopic investigations. All the results supported that the major binding mode of AOMan and ctDNA was intercalation. These studies were helpful for better understanding the interaction of AOMan with ctDNA, and beneficial to the design of new DNA targeted drugs.

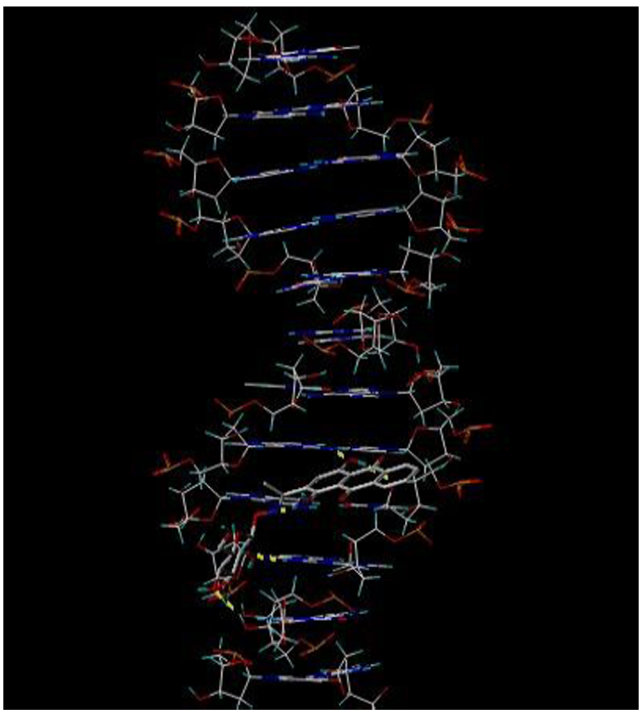

Fig. 9 Computational docking model of the binding of AOMan to ctDNA

Acknowledgments Authors are grateful to the National Natural Science Foundation of China (30970696, 20672031), Key Project of Henan Ministry of Education (14A150018), Key Programs of Henan for Science and Technology Development (142102310273), PCSIRT (IRT1061), and the Program for Innovative Research Team in University of Henan Province (2012IRTSTHN006).

References

1. Wang JC (1996) DNA topoisomerases. Annu Rev Biochem 65:635–692
2. Capranico G, Butelli E, Zunino F (1995) Change of the sequence specificity of daunorubicin-stimulated topoisomerase II DNA cleavage by epimerization of the amino group of the sugar moiety. Cancer Res 55:312–317
3. Geng SG, Cui YR, Liu QF, Cui FL, Zhang GS, Chi YW, Peng H (2013) Spectroscopic and molecular modeling study on the interaction of ctDNA with 3′-deoxy-3’-azido doxorubicin. J Lumin 141: 144–149
4. Ni YN, Wei M, Kokot S (2011) Electrochemical and spectroscopic study on the interaction between isoprenaline and DNA using multivariate curve resolution-alternating least squares. Int J Biol Macromol 49:622–628
5. Zhang XY, Wang Y, Zhang QR, Yang ZS (2010) The interaction of taurine–salicylaldehyde schiff base copper (II) complex with DNA and the determination of DNA using the complex as a fluorescence probe. Spectrochim Acta part A 77:1–5
6. Hu Z, Tong CL (2007) Synchronous fluorescence determination of DNA based on the interaction between methylene blue and DNA. Anal Chim Acta 587:187–193
7. Zhang SF, Sun XJ, Jing ZH, Qu FL (2011) Spectroscopic analysis on the resveratrol-DNA binding interactions at physiological pH. Spectrochim Acta Part A 82:213–216
8. Guin PS, Mandal PC, Das S (2012) The binding of a hydroxy-9,10-anthraquinone Cu^{II} complex to calf thymus DNA: electrochemistry and UV/Vis spectroscopy. Chem Plus Chem 77:361–369
9. Liang G, Li T, Li XH, Liu XH (2013) Electrochemical detection of the amino-substituted naphthalene compounds based on intercalative interaction with hairpin DNA by electrochemical impedance spectroscopy. Biosens Bioelectron 48:238–243
10. Liu XR, Li JH, Zhang Y, Ge YS, Tian FF, Dai J, Jiang FL, Liu Y (2011) Mitochondrial permeability transition induced by different concentrations of zinc. J Membrane Biol 244:105–112
11. Liu Y, Chen M, Cao T, Sun Y, Li CY, Liu Q, Yang TS, Yao LM, Feng W, Li FY (2013) A cyanine-modified nanosystem for in vivo upconversion luminescence bioimaging of methylmercury. J Am Chem Soc 135:9869–9876
12. Hu RR, Lam JWY, Liu Y, Zhang X, Tang BZ (2013) Aggregation-induced emission of tetraphenylethene–hexaphenylbenzene adducts: effects of twisting amplitude and steric hindrance on light emission of nonplanar fluorogens. Chem Eur J 19:5617–5624

13. Li CY, Liu Y, Wu YQ, Sun Y, Li FY (2013) The cellular uptake and localization of non-emissive iridium(III) complexes as cellular reaction-based luminescence probes. Biomaterials 34:1223–1234
14. Sirajuddin M, Ali S, Badshah A (2013) Drug–DNA interactions and their study by UV–Visible, fluorescence spectroscopies and cyclic voltametry. J Photochem Photobiol 124:1–19
15. Wang GK, Wu HW, Wang DC, Yan CL, Lu Y (2013) Exploring the binding mechanism of phosphoramidate derivative with DNA: Spectroscopy, calorimetry and modeling. Spectrochim Acta Part A 104:492–496
16. Moghaddam FG, Kompany-Zareh M, Gholami S (2012) Study of neutral red interaction with DNA by resolution of rank deficient multi-way fluorescence data. J Pharm Biomed Anal 70:388–395
17. Jana B, Senapati S, Ghosh D, Bose D, Chattopadhyay N (2012) Spectroscopic exploration of mode of binding of ctDNA with 3-hydroxyflavone: a contrast to the mode of binding with flavonoids having additional hydroxyl groups. J Phys Chem B 116:639–645
18. Marty R, N'soukpoé-Kossi CN, Charbonneau D (2009) Weinert CM, Kreplak L, Tajmir-Riahi HA, Structural analysis of DNA complexation with cationic lipids. Nucl Acid Res 37:849–857
19. Nafisi S, Norouzi Z (2009) A comparative study on the interaction of cis-and trans-platin with DNA and RNA. DNA Cell Biol 28:469–477
20. Bi SY, Yan LL, Wang Y, Pang B, Wang TJ (2012) Spectroscopic study on the interaction of eugenol with salmon sperm DNA in vitro. J Lumin 132:2355–2360
21. Li Y, Yang ZY, Li TR, Liu ZC, Wang BD (2011) Synthesis, characterization, DNA binding properties and antioxidant activity of Ln (III) complexes with schiff base ligand derived from 3-carbaldehyde chromone and aminophenazone. J Fluoresc 21:1091–1102
22. Satyanarayana S, Dabrowiak JC, Chaires JB (1992) Neither Δ-nor Λ-Tris (phenanthroline) ruthenium (II) binds to DNA by classical intercalation. Biochemistry 39:9319–9324
23. Wu FY, Xiang YL, Wu YM, Xie FY (2009) Study of interaction of a fluorescent probe with DNA. J Lumin 129:1286–1291
24. Lu Y, Wang GK, Lv J, Zhang GS, Liu QF (2011) Study on the interaction of an anthracycline disaccharide with DNA by spectroscopic techniques and molecular modeling. J Fluoresc 21:409–414
25. Modukuru NK, Snow KJ, Perrin BS Jr, Thota J, Kumar CV (2005) The contributions of a long side chain to the binding affinity of an anthracene derivative to DNA. J Phys Chem B 109:11810–11818
26. Kashanian S, Dolatabadi JEN (2009) In vitro study of calf thymus DNA interaction with butylated hydroxyanisole. DNA Cell Biol 28: 535–540
27. Kashanian S, Khodaei MM, Roshanfekr H, Shahabadi N, Mansouri G (2012) DNA binding, DNA cleavage and cytotoxicity studies of a new water soluble copper (II) complex: the effect of ligand shape on the mode of binding. Spectrochim Acta Part A 86:351–359
28. Sahoo BK, Ghosh KS, Bera R, Dasgupta S (2008) Studies on the interaction of diacetylcurcumin with calf thymus-DNA. Chem Phys 351:163–169
29. Geng SG, Wu Q, Shi L, Cui FL (2013) Spectroscopic study one thiosemicarbazone derivative with ctDNA using ethidium bromide as a fluorescence probe. Int J Biol Macromol 60:288–294
30. Ghosh K, Kumar P, Tyagi N (2011) Synthesis, crystal structure and DNA interaction studies on mononuclear zinc complexes. Inorg Chim Acta 375:77–83
31. Lakowicz JR (1999) Principles of fluorescence spectroscopy, 2nd edn. Plenum Press, New York, p 237
32. Vijayalakshmi R, Kanthimathi M, Parthasarathi R, Nair BU (2006) Interaction of chromium(III) complex of chiral binaphthyl tetradentate ligand with DNA. Bioorg Med Chem 14:3300–3306
33. Ma YD, Zhang GW, Pan JH (2012) Spectroscopic studies of DNA interactions with food colorant indigo carmine with the use of ethidium bromide as a fluorescence probe. J Agric Food Chem 60: 10867–10875
34. Fotouhi L, Atoofi Z, Heravi MM (2013) Interaction of ciprofloxacin with DNA studied by spectroscopy and voltammetry at MWCNT/DNA modified glassy carbon electrode. Talanta 103:194–200
35. Zhang GW, Fu P, Pan JH (2013) Multispectroscopic studies of paeoniflorin binding to calf thymus DNA in vitro. J Lumin 134: 303–309
36. Asadi M, Safaei E, Ranjbar B, Hasani L (2005) A study on the binding of two water-soluble tetrapyridinoporphyrazina to copper (II) complexes to DNA. J Mol Struct 754:116–123
37. Das S, Kumar GS (2008) Molecular aspects on the interaction of phenosafranine to deoxyribonucleic acid: model for intercalative drug-DNA binding. J Mol Struct 872:56–63
38. Kashanian S, Khodaei MM, Pakravan P, Adibi H (2012) Molecular aspects on the interaction of isatin-3-isonicotinylhydrazone to deoxyribonucleic acid: model for intercalative drug-DNA binding. Mol Biol Rep 39:3853–3861
39. Catalán M, Álvarez-Lueje A, Bollo S (2010) Electrochemistry of interaction of 2-(2-nitrophenyl)-benzimidazole derivatives with DNA. Bioelectrochemistry 79:162–167
40. Cai CQ, Chen XM, Ge F (2010) Analysis of interaction between tamoxifen and ctDNA in vitro by multi-spectroscopic methods. Spectrochim Acta Part A 76:202–206
41. Fei Y, Lu G, Fan G, Wu Y (2009) Spectroscopic studies on the binding of a new quinolone antibacterial agent: sinafloxacin to DNA. Anal Sci 25:1333–1338
42. Cui FL, Huo RN, Hui GQ, Lv XX, Jin JH, Zhang GS, Xing WW (2011) Study on the interaction between aglycon of daunorubicin and calf thymus DNA by spectroscopy. J Mol Struct 1001:104–110
43. Chen QY, Li DH, Zhao Y, Yang HH, Zhu QZ, Xu JG (1999) Interaction of a novel red-region fluorescent probe, Nile Blue, with DNA and its application to nucleic acids assay. Analyst 124:901–906